Preprints (www.preprints.org) | NOT PEER-REVIEWED | Posted: 12 July 2021 doi:10.20944/preprints202107.0262.v1

Generating the triangulations of the torus with the vertex-labeled graph $K_{2,2,2,2}$

S. Lawrencenko, A. M. Magomedov

Abstract: Using the orbit decomposition, a new enumerative polynomial $P(x)$ is introduced for abstract (simplicial) complexes of a given type, e.g., trees with a fixed number of vertices or triangulations of the torus with a fixed graph. The polynomial has the following useful properties:
(I) $M(1)$ is equal to the number of unlabeled complexes (of a given type),
(II) the derivative $M'(1)$ is equal to the number of non-trivial automorphisms over all unlabeled complexes,
(III) the integral of $P(x)$ from 0 to 1 is equal to the number of vertex-labeled complexes, divided by the order of the acting group.
The enumerative polynomial $P(x)$ is demonstrated for trees, and then is applied to triangulations of the torus with the vertex-labeled complete four-partite graph $G = K_{2,2,2,2}$, in which specific case $P(x) = x^{31}$. The graph G embeds on the torus as a triangulation, $T(G)$. The automorphism group of G naturally acts on the set of triangulations of the torus with the vertex-labeled graph G. For the first time, by a combination of algebraic and symmetry techniques, all vertex-labeled triangulations of the torus (twelve in number) with the graph G are classified intelligently without using computing technology, in a uniform and systematic way. It is helpful to notice that the graph G can be converted to the Cayley graph of the quaternion group Q_8 with three quaternions, i, j, k, as generators.

Keywords: group action; orbit decomposition; polynomial; graph; tree; triangulation; torus; automorphism; quaternion group

1 Introduction

This article is an extended version of the talk given by the first author at the Minisymposium "Graphs, Polynomials, Surfaces, and Knots", the 8th European Congress of Mathematics, on 22 June 2021.

In labeled graph enumeration problems, the vertices of the graph are labeled so as to be distinguishable from each other, while in unlabeled enumeration problems

Preprints (www.preprints.org) | NOT PEER-REVIEWED | Posted: 12 July 2021 doi:10.20944/preprints202107.0262.v1

any admissable permutation of the vertices is regarded as producing the same graph, so the vertices are considered unlabeled. In general, labeled problems are usually easier than unlabeled ones. For instance, Cayley's tree formula [**?**, **?**] gives the number, n^{n-2}, of trees with n vertices bijectively labeled by $1,\ldots,n$, whereas the number of unlabeled trees with n vertices can only be evaluated as the coefficients of a generating function [**?**]. The number n^{n-2} can be interpreted as the number of different ways of placing n folders on the desktop into the one chosen out of them. The orbit decomposition [**?**] is an important tool for reducing unlabeled problems to labeled ones: Each unlabeled class is considered as a symmetry class, or an isomorphism class, of labeled graphs. In the current paper we introduce a new enumerative polynomial $P(x)$ which enables us to enumerate discrete structures in both labeled and unlabeled settings.

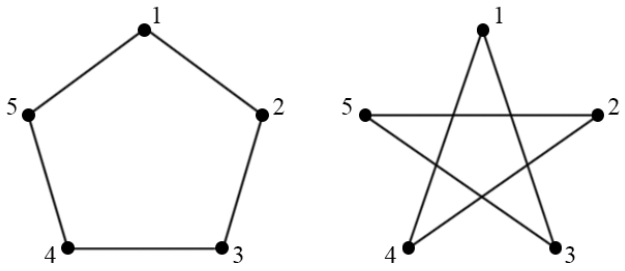

Figure 1. A pair of complementary graphs isomorphic to C_5.

Vertex-unlabeled graphs are considered up to isomorphism. For example, all cycles of length 5 are isomorphic and thus represent the same unlabeled graph, C_5, up to isomorphism. The vertices of this graph can be assigned labels 1, 2, 3, 4, 5 in twelve different ways. Furthermore, the twelve different labeled graphs split into six pairs of graphs which are the complementarities of each other (in each pair); one such pair is shown in Figure 1. (See Remark 1 in Section 6.)

Two triangulations with the same vertex-labeled graph are considered different provided one has a face determined by some three vertices with specific labels while the other does not. For instance, the two triangulations in the upper row of Figure 8(b) are different because the one in the left-hand side has a face with vertices 1, j, k while the one in the right-hand side does not. The reader may notice that the two triangulations have no (2-)faces in common and that they are complemenraty of each other as labeled 2-complexes just like the complementary graphs in Figure 1 have no 1-faces (edges) in common. On the other hand, the two triangulations represent the same unlabeled triangulation, the 8-vertex 6-regular triangulation, $T(G)$, of the torus which is known [**?**, **?**] to be unique, up to isomorphism, triangular embedding of the complete 4-partite graph $G = K_{2,2,2,2}$ on the torus (see Figure 2, left, identify the sides of the rectangle, in pairs, to obtain a torus). Two triangulations are called *isomorphic* provided there is a bijection between their vertex sets, which sends edges to edges and faces to faces.

Preprints (www.preprints.org) | NOT PEER-REVIEWED | Posted: 12 July 2021 doi:10.20944/preprints202107.0262.v1

The results of the current paper are primarily concerned with the symmetry properties of the graph $G = K_{2,2,2,2}$ and the triangulation $T(G)$. The importance and significance of the graph G are justified by the fact that G is the 1-skeleton of the four-dimensional regular cross polytope, or the 16-cell, which is one of the six regular convex 4-polytopes. Also, the triangulation $T(G)$ is known [**?**, **?**] as one of the twenty-one irreducible triangulations of the torus. Furthermore, $T(G)$ can be realized geometrically [**?**] as a toroidal polyhedral suspension in $\mathbb{R}^3$, as shown in Figure 2 (right), and as a nobel polyhedron in $\mathbb{R}^4$, whose properties are studied extensively in [**?**]. As the main result of the current paper, it is shown (Section 6) how to generate all labeled triangulations of the torus with the graph G in an intelligent fashion without using computer resources. Geometrically, these labeled triangulations correspond to different (as point-sets) 2-dimensional toroidal subcomplexes of the 16-cell in $\mathbb{R}^4$. An important payoff of our approach is a unified view of algebra and symmetry studies to address combinatorial questions in topologucal graph theory and geometry.

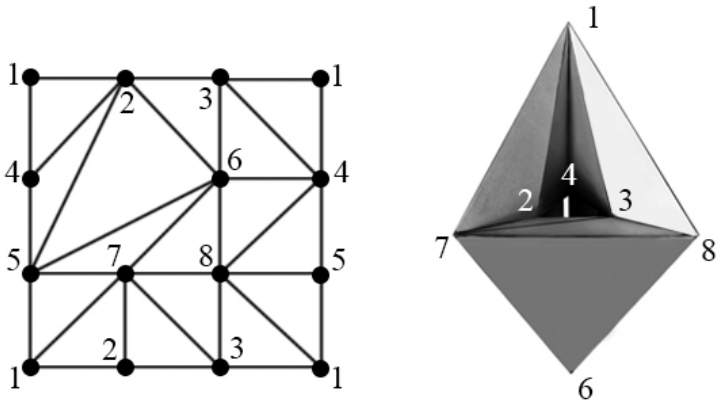

Figure 2. Triangulation $T(G)$ of the torus with the graph $G = K_{2,2,2,2}$.

2 Preliminary: The orbit decomposition

In this section a general theory is presented. The reader will find specific and practical examples in Section 4.

In the general case, let Ω be a fixed finite set of unlabeled discrete substructures of an ambient structure $\mathscr{K}$. For the sake of certainty, the set Ω, $= \Omega^n$, can be thought of as a set of spanning unlabeled (that is, considered up to isomorphism) subcomplexes of some ambient n-vertex unlabeled simplicial complex $\mathscr{K}$. Let K be a spanning simplicial subcomplex of $\mathscr{K}$. An *automorphism* of K is any permutation of the vertex set of $\mathscr{K}$ which sends d-faces of K onto d-faces of K, for any d. Let Ω_k^n be the set of unlabeled n-vertex k-symmetric subcomplexes of $\mathscr{K}$, where the term "k-symmetric" means that the automorphism group of the subcomplex has order k.

Preprints (www.preprints.org) | NOT PEER-REVIEWED | Posted: 12 July 2021 doi:10.20944/preprints202107.0262.v1

Thus,

$$|\Omega^n| = \sum_k |\Omega^n_k|.$$

In this paper, the two main instances of Ω^n are as follows:
(i) the set of n-vertex trees (Section 4) and
(ii) the set of triangulations of the torus with the 8-vertex graph $G = K_{2,2,2,2}$ (Sections 5, 6).

Let Λ^n be the set obtained from the set Ω^n by labeling the n vertices of each element of Ω^n with labels $1,\ldots,n$ bijectively, in all combinatorially different ways. For $K \in \Omega^n$, two vertex labelings of K are considered different provided there is a face of K with vertices with specific labels in one labeling of K but there is no face of K with the same set of labels in the other labeling. For example, Figure 4(a) shows all pairwise different vertex labelings of a 4-vertex path of length 3 with labels $1,2,3,4$. Let Λ^n_k be the subset of Λ^n whose elements are k-symmetric (as unlabeled simplicial complexes).

Let $\Gamma = \mathrm{Aut}(\mathscr{K})$ be the automorphism group of the ambient complex $\mathscr{K}$. Thus, Γ is a subgroup of the symmetric group S_n and acts naturally on the set Λ^n. It is clear that under the action the following three statements hold for any $K \in \Lambda$:
(1) The stabilizer subgroup of K is identical with the automorphism group $\mathrm{Aut}(K)$,
(2) the size of the orbit of K is equal to the number of different vertex labelings of K,
(3) the total number of orbits is equal to $|\Omega^n|$.

Let $K \in \Omega^n_k$. By the orbit-stabilizer theorem [**?**], the size of the orbit of K is equal to the index $|\Gamma|/k$ of the stabilizer subgroup of K in the group Γ. Summing over $K \in \Omega^n_k$ gives the following:

$$|\Lambda^n_k| = \frac{|\Gamma|}{k}|\Omega^n_k|. \tag{1}$$

Futhermore, we can sum Eqs. (1) over divisors k of $|\Gamma|$, possibly with multiplicities (for instance, multiplicity 2 occurs for $k = 2$ in the case of trees with 5 vertices, Section 4). Summing Eqs. (1) over k gives the following:

$$\sum_{k\,||\Gamma|} |\Lambda^n_k| = \sum_{k\,||\Gamma|} \frac{|\Gamma|}{k}|\Omega^n_k|. \tag{2}$$

Thus, we come to the orbit decomposition formula [**?**] for the action of the group Γ on the set Λ^n:

$$|\Lambda^n| = \sum_{i=1}^{|\Omega^n|} \frac{|\Gamma|}{|\mathrm{Aut}(K_i)|},$$

where $\mathrm{Aut}(K_i)$ stands for the automorphism group of any representative element K_i in the orbit i.

Preprints (www.preprints.org) | NOT PEER-REVIEWED | Posted: 12 July 2021 doi:10.20944/preprints202107.0262.v1

When it is clear what value n is meant to be, the notations Ω_k^n and Λ_k^n may be abbreviated to Ω_k and Λ_k, respectively.

3 The enumerative polynomial

For a given set Ω $(= \Omega^n)$, we define our enumerative polynomial by

$$P(x)(= P_n(x)) = \sum_{k\,||\Gamma|} |\Omega_k| x^{k-1}. \tag{3}$$

Evaluating at $x = 1$ gives

$$P(1) = |\Omega|.$$

The enumerative polynomial defined by Eq. (3) has smart derivatives and integral. Evaluate the derivative:

$$P'(x) = \sum_{k\,||\Gamma|} (k-1)|\Omega_k| x^{k-2}.$$

$$P'(1) = \sum_{k\,||\Gamma|} (k-1)|\Omega_k| = \sum_{k\,||\Gamma|} k|\Omega_k| - |\Omega|.$$

Therefore,

$$P'(1) = \tilde{\alpha} = \alpha - \bar{\alpha},$$

where α is the total number of automoirphisms, $\bar{\alpha}$ is the number of trivial automorphisms, and $\tilde{\alpha}$ is the number of nontrivial automorphisms over Ω.

Evaluate the integral:

$$\int_0^1 P(x)dx = \sum_{k\,||\Gamma|} \frac{1}{k}|\Omega_k|.$$

Thus, by Eq. (2):

$$|\Gamma| \int_0^1 P(x)dx = \sum_{k\,||\Gamma|} \frac{|\Gamma|}{k}|\Omega_k| = \sum_{k\,||\Gamma|} |\Lambda_k| = |\Lambda|.$$

Thus,

$$\int_0^1 P(x)dx = \frac{|\Lambda|}{|\Gamma|}.$$

Summarizing, we come to the following result.

Preprints (www.preprints.org) | NOT PEER-REVIEWED | Posted: 12 July 2021 doi:10.20944/preprints202107.0262.v1

Theorem 1. *The enumerative polynomial* $P(x) = \sum_{k\,||\Gamma|} |\Omega_k| x^{k-1}$ *has the following three properties:*
(a) $P(1) = |\Omega|$,
(b) $P'(1) = \tilde{\alpha}$, *the number of nontrivial automorphisms over* Ω,
(c) $\int_0^1 P(x)dx = |\Lambda|/|\Gamma|$. □

4 Examples: Trees

In this section we demonstrate the concept of the enumerative polynomial in a simple framework. Specifically for trees on n ($n \geqslant 4$) vertices, the ambient simplicial complex $\mathscr{K}$ is the complete graph K_n, the acting group Γ is the symmetric group S_n, and the enumerative polynomial is given by

$$P_n(x) = \sum_{k\,|\,n!} |\Omega_k| x^{k-1}.$$

Figure 3. Non-isomorphic trees with 4 vertices, T_1 (left) and T_2 (right).

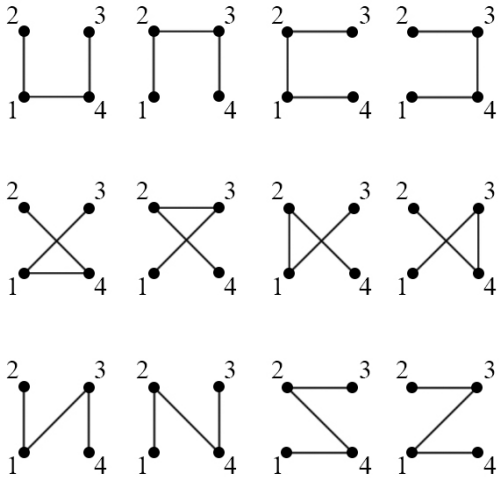

Figure 4(a). All vertex labelings of the tree T_1.

1. *Trees with 4 vertices*

Figure 3 shows two non-isomorphic 4-vertex trees, T_1 (left) and T_2 (right). It is known [**?**] that $\Omega^4 = \{T_1, T_2\}$. The automorphism groups of T_1 and T_2 are the

Preprints (www.preprints.org) | NOT PEER-REVIEWED | Posted: 12 July 2021 doi:10.20944/preprints202107.0262.v1

symmetric groups S_2 and S_3 having orders 2 and 6, respectively. Thus,

$$P_4(x) = x^{2-1} + x^{6-1} = x^5 + x, \qquad P_4(1) = 2, \qquad P_4'(1) = 6, \qquad \int_0^1 P_4(x)dx = \frac{2}{3}.$$

Thus, by Theorem 1:

$|\Omega_4| = P_4(1) = 2$,
$\tilde{\alpha}_4 = P_4'(1) = 6$,
$|\Lambda_4| = (\int_0^1 P_4(x)dx) \cdot 4! = 16 = 4^{4-2}$ (which agrees with Cayley's formula for the number of vertex-labeled trees).

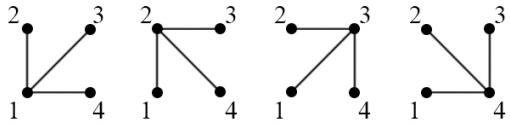

Figure 4(b). All vertex labelings of the tree T_2.

The 16 labeled trees on 4 vertices are shown in Figures 4 (a), (b). By Eq. (2), the more automorphisms a tree has the fewer copies of that tree there are in the ambient graph.

2. *Trees with 5 vertices*

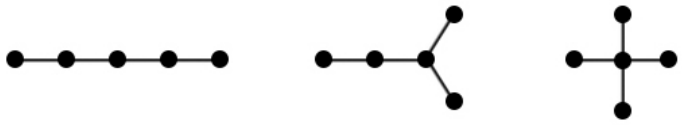

Figure 5. All pairwise non-isomorphic trees with 5 vertices.

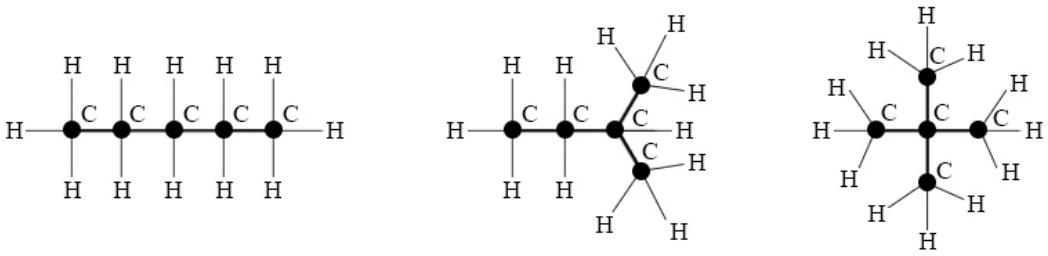

Figure 6. Pentane, isopentane, neopentane (from left to right).

Figure 5 shows three pairwise non-isomorphic 5-vertex trees, T_1 (left), T_2 (middle), and T_3 (right). It is known [**?**] that $\Omega^5 = \{T_1, T_2, T_3\}$. The automorphism groups of T_1, T_2, T_3 are the symmetric groups S_2, S_2, S_4 having orders 2, 2, 24, respectively. Thus:

$$P_5(x) = x^{2-1} + x^{2-1} + x^{24-1} = x^{23} + 2x, \qquad P_5'(x) = 23x^{22} + 2,$$

Preprints (www.preprints.org) | NOT PEER-REVIEWED | Posted: 12 July 2021 doi:10.20944/preprints202107.0262.v1

$$P_5(1) = 3, \qquad P_5'(1) = 25, \qquad \int_0^1 P_5(x)dx = \frac{25}{24}.$$

Thus, by Theorem 1:

$|\Omega_5| = P_5(1) = 3$,
$\tilde{\alpha}_5 = P_5'(1) = 25$,
$|\Lambda_5| = (\int_0^1 P_5(x)dx) \cdot 5! = \frac{25}{24} \cdot 120 = 125 = 5^{5-2}$ (which agrees with Cayley's formula for the number of vertex-labeled trees).

On the practical side, trees provide models for saturated acyclic hydrocarbons [**?**]. The number of different chemical isomers sharing the same chemical formula $C_n H_{2n+2}$ is equal to the number of pairwise non-isomorphic trees on n vertices. For $n = 5$, all pairwise non-isomorphic trees with 5 vertices are shown on Figure 5, and the corresponding isomers of non-cyclic alkanes with the formula $C_5 H_{12}$ are listed in Figure 6: pentane, isopentane, neopentane (from left to right).

In conclusion of this section, we mention Bernstein's theorem [**?**] restricted to the real axis, which states: $|M'(1)| \leqslant \deg M(x) \cdot |M(1)|$ for any polynomial $M(x)$. It is tempting to apply this inequality to the enumerative polynomial $P_n(x)$ along with its derivative and integral, but it only produces simple corollaries. For instance, apply Bernstein's theorem to the polynomial $M(x) = \int_0^x P_n(t)dt$ in the set Ω^n of pairwise non-isomorphic trees on n unlabeled vertices ($n \geqslant 4$). Since it can be easily seen that the largest order of the automorphism group of an n-vertex tree is $(n-1)!$, it follows that $\deg M(x) \leqslant (n-1)!$ and, by Bernstein's theorem, $|M'(1)| = P_n(1) \leqslant (n-1)! \int_0^1 P_n(x)dx$. Thus, by Theorem 1 (a), (c), we come to the following inequality: $|\Omega^n| \leqslant |\Lambda^n|/n$. Now, applying Cayley's tree formula, $|\Lambda^n| = n^{n-2}$, we come to the following upper bound on the number of trees with n unlabeled vertices: $|\Omega^n| \leqslant n^{n-3}$.

5 The Cayley graph of Q_8

In the remainer of this paper, $T(G)$ stands for the triangulation of the torus shown in Figure 2 and G ($= K_{2,2,2,2}$) stands for its graph, discussed in the Introduction.

It can be verified [**?**, **?**] that the triangulation $T(G)$ is the only irreducible triangulation of the torus whose graph is isomorphic to $K_{2,2,2,2}$, whence all embeddings of G on the torus are isomorphic as triangulations. Thus, the set Ω of all non-isomorphic triangulations of the torus, with the graph G, consists of a single element: $\Omega = \{T(G)\}$.

The automorphism group $\mathrm{Aut}(G)$ of the graph G is identical with the automorphism group of its complementary graph $\mathrm{Aut}(\overline{G}) \equiv \mathrm{Aut}(4K_2)$, which is identical with the composition (or wreath product) $S_4[\mathrm{Aut}(K_2)] = S_4[S_2]$ (see [**?**]) and has order $|S_4| \cdot |S_2|^4 = 4! \cdot (2!)^4 = 384$.

Preprints (www.preprints.org) | NOT PEER-REVIEWED | Posted: 12 July 2021 doi:10.20944/preprints202107.0262.v1

Let the group $\Gamma = \mathrm{Aut}(G)$ act naturally on the set $\Lambda = \Lambda^8$ of triangulations of the torus with the 8-vertex-labeled graph G; under this action, each automorphism $\gamma \in \mathrm{Aut}(G)$ simply replaces each vertex label u by $\gamma(u)$. (Geometrically, the ambient simplicial complex $\mathscr{K}$ may be thought of as the 2-skeleton of the 16-cell in $\mathbb{R}^4$ as discussed at the end of the Introduction.) Since $\Omega = \{T(G)\}$, all toroidal triangulations with the vertex-labeled graph G are in a single orbit under the action of $\Gamma = \mathrm{Aut}(G)$ on Λ. The automorphism group $\mathrm{Aut}(T(G))$ of the triangulation $T(G)$ is determined in [**?**, **?**]. This group can be generated by the involutions $\tau_1 = (35)(47)$ and $\tau_2 = (16)(37)(45)$ together with the cyclic automorphism $\tau_3 = (15276384)$ (check with Figure 2, left). Thus, $|\mathrm{Aut}(T(G))| = 2 \cdot 2 \cdot 8 = 32$, whence $|\Omega| = |\Omega_{32}| = 1$. Summarizing, the enumerative polynomial (3) for the set $\Omega = \{T(G)\}$ can be written down as follows:

$$P(x) = \sum_{k \,|\, |\mathrm{Aut}(G)|} |\Omega_k| x^{k-1} = |\Omega_{32}| x^{31} = x^{31}.$$

Thus, by Theorem 1(c),

$$\frac{1}{32} = \int_0^1 x^{31} dx = \frac{|\Lambda|}{|\mathrm{Aut}(G)|} = \frac{|\Lambda|}{384},$$

whence the number of triangulations of the torus with the vertex-labeled graph G is equal to 12:

$$|\Lambda| = \frac{384}{32} = 12. \tag{4}$$

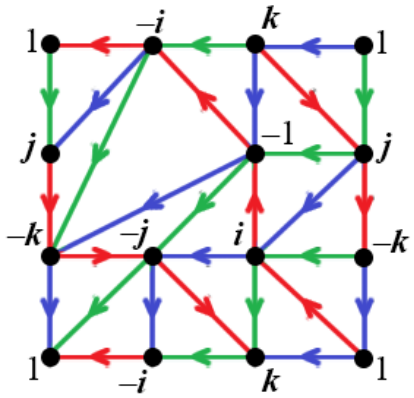

Figure 7. The Cayley graph G of Q_8.

The crucial idea is to convert the graph G (Figure 2, left) into the Cayley graph of the quaternion group Q_8 by first replacing the labels 1, 2, 3, 4, 5, 6, 7, 8 with the quaternions 1, $-i$, k, j, $-k$, -1, $-j$, i (respectively) and then assigning colors and directions to the edges as shown in Figure 7. This conversion will enable us to classify the 12 different triangulations (Section 6), which number is stated by Eq. (4), in a systematic way by a combination of algebraic and symmetry techniques.

Preprints (www.preprints.org) | NOT PEER-REVIEWED | Posted: 12 July 2021 doi:10.20944/preprints202107.0262.v1

The red [respectively, green, blue] arrows correspond to the multiplication by i (always on the right) [replectively, by j, k]; for instance, $k \cdot j = -i$ (check with Figure 7).

It should be noted that the Cayley graph, in fact, depends on the choice of the group generators, and what is often called the Cayley graph of Q_8 is the subgraph obtained from Figure 7 by deleting the blue edges. This subgraph corresponds to the set $\{i, j\}$ chosen as a *minimal* generating set. Furthermore, this subgraph is known [**?**] to quadrangulate the torus, and it can be thought of that the quadrilaterals are dissected into triangles by the blue edges as in Figure 7; the resulting graph triangulates the torus and is called the (extended) Cayley graph of the quaternion group Q_8 throughout this paper.

We finally make a useful observation. The edge set of the graph G forms a single orbit under the natural action of the group $\Gamma \equiv \mathrm{Aut}(G)$; however, there are two orbits under the action of $\mathrm{Aut}(T(G))$ (as a subgroup of Γ). In the latter instance, one orbit has 8 edges and the other one has 16 edges, where the orbit of size 8 coinsides with the edge set of the union of two disjoint red cycles of length 4 (Figure 7). This can be proved by straightforward inspection of the three generators of $\mathrm{Aut}(T(G))$ as follows: The generator $\tau_1 = (j\ {-j})(k\ {-k})$ preserves each of the three colors, while the generators $\tau_2 = (1\ {-1})(j\ {-k})(k\ {-j})$ and $\tau_3 = ({-k}\ {-i}\ {-j}\ {-1}\ k\ i\ j\ 1)$ preserve the red color, changing green into blue and blue into green (check with Figure 7). Therefore, the representation of the graph G as a triangulation $T(G)$ of the torus (Figure 2, left) has an advantage before the graph G only as itself: The combinatorial structure of the triangulation $T(G)$ alone distinguishes the edges that are colored red in Figure 7. (Observe from Figure 7 that the two red cycles are both geodetic and homotopic to each other on the torus; a *geodetic cycle* C in a graph H is a cycle with the property that for every two vertices $u, v \in C$ at least one of the paths uCv or vCu is a geodesic in H.)

6 Systematic generation of toroidal triangulations with the graph $G = K_{2,2,2,2}$

Explicit identification of the 12 triangulations of the torus with the graph $G = K_{2,2,2,2}$ was done by an exhaustive computer search in [**?**]. In this section it is shown how to generate the 12 triangulations intelligently without using computing technology. We use the representation of G in Figure 7 instead of the representation in Figure 2 (left). It should be noted that we regard the Cayley graph in Figure 7 as just another vertex labeling of the original vertex-labeled simple graph G in Figure 2 (left) and use the same notation for both graphs. The edge colors and directions will only help us to reveal the structure of the set Λ.

Consider the following four permutations of the vertex set of the graph G (leav-

Preprints (www.preprints.org) | NOT PEER-REVIEWED | Posted: 12 July 2021 doi:10.20944/preprints202107.0262.v1

ing the rest of the vertices fixed):

$$\text{id}, \qquad \gamma_{\text{rot}} = (1\ \ i\ \ {-1}\ \ {-i}),$$

$$\gamma_{\text{ref}} = (1\ \ {-1}), \qquad \gamma_{\text{rot}}\gamma_{\text{ref}} = (1\ \ {-i})(i\ \ {-1}).$$

It is not hard to verify with Figure 7 that each the four permutations is an automorphism of the graph G but not each of them is an automorphism of the triangulation $T(G)$: While id is the (identity) automorphism of $T(G)$, none of γ_{rot}, γ_{ref}, or $\gamma_{\text{rot}}\gamma_{\text{ref}}$ is an automorphism of $T(G)$. The notation is inspired by the observation that the graph automorphism γ_{rot} is realized geometrically as a rotation of the square with vertices 1, i, -1, $-i$ while the graph automorphisms γ_{ref} and $\gamma_{\text{rot}}\gamma_{\text{ref}}$ are realized geometrically as (axial) reflections of that square as indicated by the self-explanatory pictures in the left-hand sides of the frames of Figure 8(a).

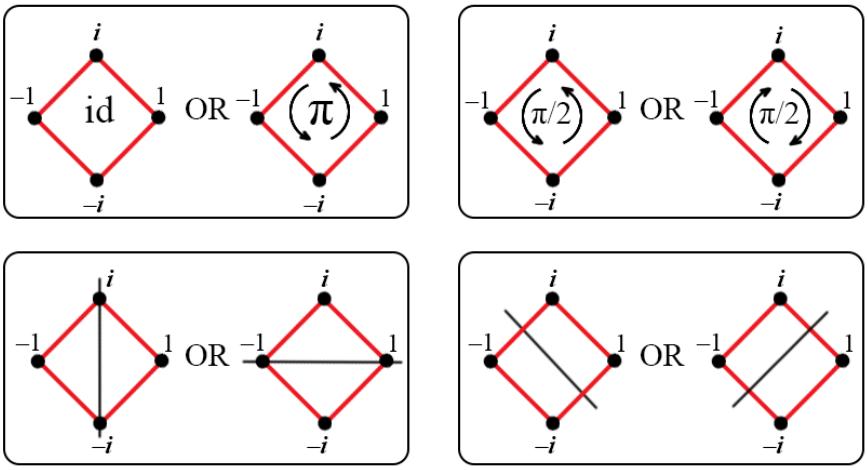

Figure 8(a). The images in the left-hand sides of the frames correspond to: id, γ_{rot}, respectively (upper row) and γ_{ref}, $\gamma_{\text{rot}}\gamma_{\text{ref}}$, respectively (lower row).

For $\gamma \in \Gamma = \text{Aut}(G)$, let $\gamma(T(G))$ denote the triangulation to which γ sends $T(G)$ under the action of the group Γ on the set Λ of vertex-labeled toroidal triangulations with the graph G. It is not hard to verify with Figure 7 that the four triangulations $T(G)$, $\gamma_{\text{rot}}(T(G))$, $\gamma_{\text{ref}}(T(G))$, and $\gamma_{\text{rot}}\gamma_{\text{ref}}(T(G))$ (Figure 8(b)) are pairwise different. Moreover, the pair of triangulations in each row of Figure 8(b) have no faces in common at all.

Denote by $D_8 = D_8(1, i, -1, -i)$ the dihedral group (often denoted by D_4 in geometry) regarded as the automorphism group of the (red) cycle $(1, i, -1, -i)$ of G. Consider the action of this group (as a subgroup of $\Gamma = \text{Aut}(G)$) on the set Λ, fixing the other four vertices of G (that is, j, $-j$, k, and $-k$). All eight elements of D_8 are shown geometrically in Figure 8(a). It is not hard to verify that the graph automorphisms appearing in one frame (Figure 8(a)) produce the same effect on

Preprints (www.preprints.org) | NOT PEER-REVIEWED | Posted: 12 July 2021 doi:10.20944/preprints202107.0262.v1

$T(G)$ under the action of D_8 on Λ, that is, both graph automorphisms send $T(G)$ to the same triangulation.

Let $D_8/Z(D_8)$ denote the quotient group of the dihedral grioup $D_8(1, i, -1, -i)$ by its center $Z(D_8)$. This factorization is illustrated in Figure 8(a), in which the elements of the quotient group $D_8/Z(D_8)$ are four pairs of similar graph automorphisms aggregated into the four frames of Figure 8(a). (The quotient group $D_8/Z(D_8)$ acts faithfully on Λ.) We thus obtain Series 1 of four pairwise different triangulations of the torus with the graph G:

Lemma 1. *Under the action of the quotient group $D_8/Z(D_8)$ of the dihedral group $D_8 = D_8(1, i, -1, -i)$ by its center on the set Λ, the orbit of the triangulation $T(G)$ consists of the four vertex-labeled triangulations shown in Figure 8(b) as Series 1. Moreover, the pairs of triangulations appearing in the same row of Figure 8(b) do not have any common faces at all; they are complementary of each other as simplicial 2-complexes with the same graph G.* □

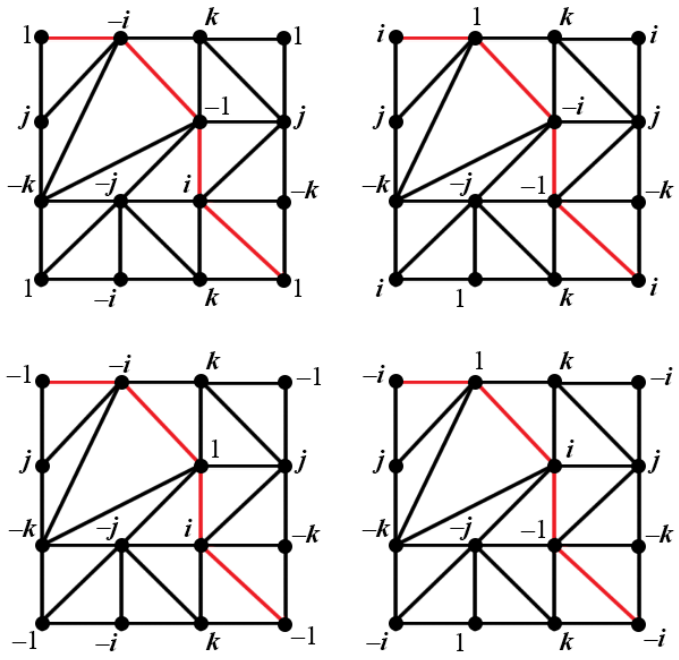

Figure 8(b). Pairwise different labeled triangulations: Series 1:
$T(G)$ and $\gamma_{\mathrm{rot}}(T(G))$, respectively (upper row),
$\gamma_{\mathrm{ref}}(T(G))$ and $\gamma_{\mathrm{rot}}\gamma_{\mathrm{ref}}(T(G))$, respectively (lower row).

Consider the automorphism $(i\ j)(-i\ -j)$ of the graph G. This graph automorphism moves the triangulation $T(G)$ to the triangulation $(i\ j)(-i\ -j)(T(G))$, shown in the left-hand side of the upper row of Figure 9, taking the (red) cycle $(1, i, -1, -i)$ onto the (green) cycle $(1, j, -1, -j)$ (check with Figure 7). We process the triangulation $(i\ j)(-i\ -j)(T(G))$ in the same way as we did with the triangulation $T(G)$

Preprints (www.preprints.org) | NOT PEER-REVIEWED | Posted: 12 July 2021 doi:10.20944/preprints202107.0262.v1

in the proof of Lemma 1, swapping i and j, $-i$ and $-j$, and switching from the red to the green color. This results in Series 2 of four pairwise different toroidal triangulations, shown in Figure 9. Each of them is obtained as effect of the graph automorphism $(i\ j)(-i\ -j)$ on the corresponding triangulation of Figure 8(b). The groups D_8 and $D_8/Z(D_8)$ are defined similarly as for $T(G)$ in the proof of Lemma 1.

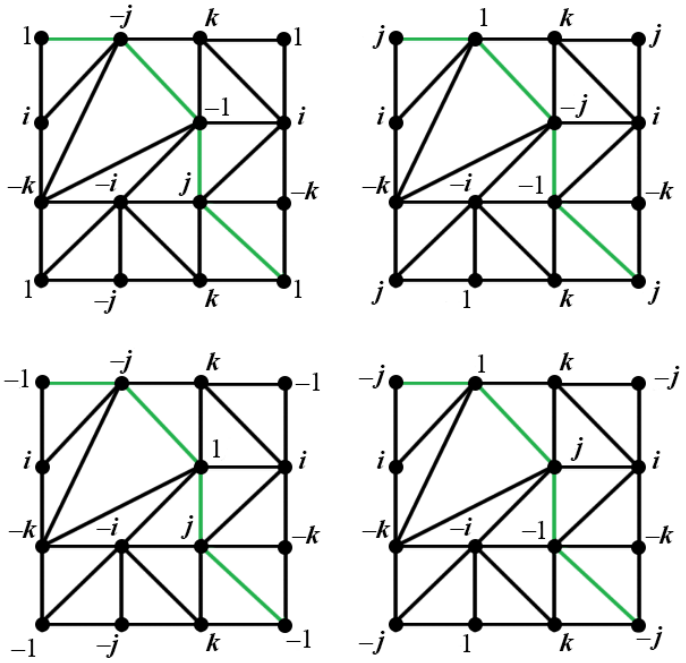

Figure 9. Pairwise different labeled triangulations: Series 2: $(i\ j)(-i\ -j)(T(G))$ and $(i\ j)(-i\ -j)(\gamma_{\text{rot}}(T(G)))$, respectively (upper row), $(i\ j)(-i\ -j)(\gamma_{\text{ref}}(T(G)))$ and $(i\ j)(-i\ -j)(\gamma_{\text{rot}}\gamma_{\text{ref}}(T(G)))$, respectively (lower row).

Similarly, the triangulation $(i\ k)(-i\ -k)(T(G))$ is presented in the left-hand side of the upper row of Figure 10, with the (blue) cycle $(1,k,-1,-k)$ in place of the (red) cycle $(1,i,-1,-i)$ in Figure 8(b). We treat the triangulation $(i\ k)$ $(-i\ -k)(T(G))$ in the same way as $T(G)$ in the proof of Lemma 1, swapping i and k, $-i$ and $-k$, and switching from the red to the blue color. The groups D_8 and $D_8/Z(D_8)$ are defined similarly as for $T(G)$ in the proof of Lemma 1. We thus obtain Series 3 of four pairwise different toroidal triangulations, shown in Figure 10.

Theorem 2. *There are precisely twelve triangulations of the torus with the vertex-labeled graph $G = K_{2,2,2,2}$, presented in Figures 8(b), 9, and 10, all isomorphic but pairwise different as vertex-labeled triangulations. They are obtained from the triangulations $T(G)$ (Figure 7), $(i\ j)(-i\ -j)(T(G))$, and $(i\ k)(-i\ -k)(T(G))$ by the action of the groups $D_8/Z(D_8)$, the quotients of the dihedral groups by their*

Preprints (www.preprints.org) | NOT PEER-REVIEWED | Posted: 12 July 2021 doi:10.20944/preprints202107.0262.v1

centers, on the set Λ*, where* D_8 *stands for the automorphism groups of the red cycle* $(1,i,-1,-i)$ *(Figure 8(a)), green cycle* $(1,j,-1,-j)$ *(Figure 9), and the blue cycle* $(1,k,-1,-k)$ *(Figure 10), respectively. Moreover, each of the six pairs of triangulations in one row of Figures 8(b), 9, and 10 do not have any common faces at all; they are complementary of each other as simplicial* 2*-complexes with the same graph G.*

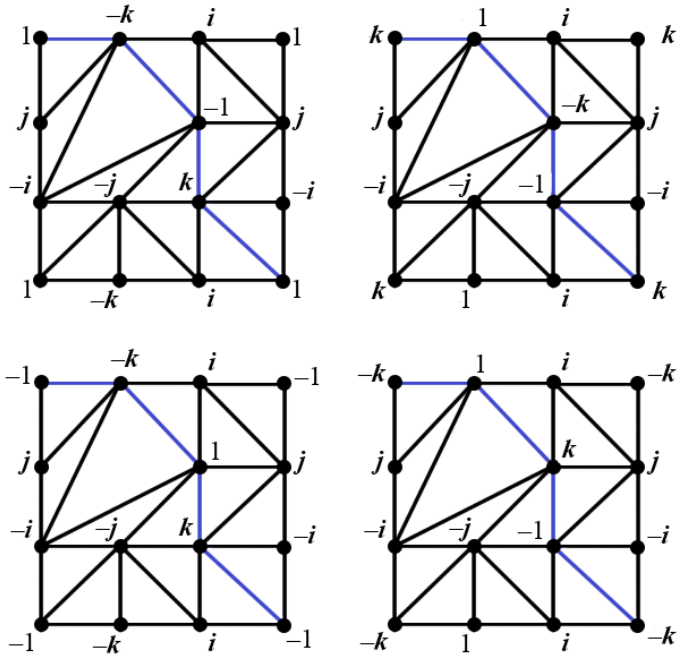

Figure 10. Pairwise different labeled triangulations: Series 3: $(i\ k)(-i\ -k)(T(G))$ and $(i\ k)(-i\ -k)(\gamma_{\text{rot}}(T(G)))$, respectively (upper row), $(i\ k)(-i\ -k)(\gamma_{\text{ref}}(T(G)))$ and $(i\ k)(-i\ -k)(\gamma_{\text{rot}}\gamma_{\text{ref}}(T(G)))$, respectively (lower row).

Proof of Theorem 2. Observe that Figure 9 [respectively, Figure 10] is obtained from Figure 8(b) by swapping i and j, $-i$ and $-j$ [respectively, i and k, $-i$ and $-k$] in each of the four diagrams, and switching from the red to the green [respectively, blue] color. Thus, analogs of Lemma 1 still hold for the dihedral groups $D_8 = D_8(1, j, -1, -j)$ and $D_8(1, k, -1, -k)$. Thus, the four triangulations in Figure 9 [respectively, Figure 10] are pairwise different as well as the four triangulations in Figure 8(b). Finally, it can be easily verified that any pair of triangulations taken from different Figures 8(b), 9 , or 10 are different as triangulations with the vertex-labeled graph G. Thus, we have identified 12 pairwise different triangulations of the torus with the graph G. There are no more different triangulations, by Eq. (4). □

Remark 1. It is not hard to verify that the cycle C_5 is the only, up to isomorphism, self-complementary graph homeomorphic to the 1-torus (that is, a circle); see Fig-

Preprints (www.preprints.org) | NOT PEER-REVIEWED | Posted: 12 July 2021 doi:10.20944/preprints202107.0262.v1

ure 1. In this specific case we have: $\mathscr{K} = K_5$, $\Gamma \equiv \mathrm{Aut}(K_5) \equiv S_5$, $\mathrm{Aut}(C_5) \equiv D_{10}$, $P(x) = x^9$, $\int_0^1 P(x)dx = 1/10$. Thus, by Theorem 1(c), $1/10 = |\Lambda|/|S_5|$, whence $|\Lambda| = 5!/10 = 12$ is the number of different vertex labelings of C_5. It is not hard to verify that those 12 different labeled graphs split into six pairs of cycles which are the complementarities of each other in each pair (see an example in Figure 1).

Thus there exist exactly 6 pairs of pairwise complementary simplicial 1-complexes homeomorphic to the 1-torus, which have a cycle of length 5 as underlying 1-complex. Analogously, $T(G)$ (Figure 2, left) is the only, up to isomorphism, self-complementary 2-complex homeomorphic to the 2-torus [**?**]. Finally, as an intriguing coincidence, there are exactly 6 pairs of pairwise complementary simplicial 2-complexes homeomorphic to the 2-torus, which have as underlying 2-complex the triangulation $T(G)$.

7 Some conclusive remarks

Our approach to studying the 8-vertex triangulation $T(G)$ of the torus with the graph $G = K_{2,2,2,2}$ (Figure 2, left) can be briefly summarized as follows. The vertex-unlabeled graph G is known to embed on the torus uniquely up to isomorphism, producing the triangulation $T(G)$. Using symmetry properties of G and $T(G)$, Theorem 1(c) enables us to calculate the number, 12, of pairwise different (triangular) embeddings of the vertex-labeled graph G on the torus. Furthermore, the algebraic approach proposed in this paper enables us to generate the 12 embeddings explicitly in the form of graphics (Figures 8(b), 9, 10), for the first time without computer assistance. For this, we think of the graph G as the (extended) Cayley graph G of the quaternion group Q_8 (Figure 7) and observe that the dihedral group $D_8/Z(D_8)$ of the automorphisms of the cycle $(1, i, -1, -i)$ factorized by its center, acting on the set Λ, moves $T(G)$ to some 4 pairwise different triangulations, including $T(G)$ itself (Figure 8(b)). We also observe that the same construction applies to the triangulations $(i\ j)(-i\ -j)(T(G))$ and $(i\ k)(-i\ -k)(T(G))$ in place of $T(G)$ (Figures 9, 10). Totally, we obtain $4 \cdot 3 = 12$ pairwise different triangulations of the torus with the vertex-labeled graph G.

As far as graph coloring topics go, we observe first that the operation of converting the graph $G = K_{2,2,2,2}$ into the Cayley graph of Q_8 (Figure 7) makes the graph *Grünbaum colored* (see a review [**?**]), which means that the edges of the graph are 3-colored so that each face of the triangulation $T(G)$ has all the three colors in its boundary edges. Moreover, observe that any cycle of G (Figure 7) with length 3 has all the 3 colors in its edges, and thus *any* triangulation with the graph G is Grünbaum colored. Observe that Grünbaum coloring entails that edges with the same color (red, for instance) are never neighboring around any vertex of the triangulation, which prevents us from algebraic meaninglessness; for example, it prevents the vertices x and $x \cdot i \cdot i$ $(= -x)$ from being adjacent in G, for any $x \in Q_8$;

Preprints (www.preprints.org) | NOT PEER-REVIEWED | Posted: 12 July 2021 doi:10.20944/preprints202107.0262.v1

see Figure 11.

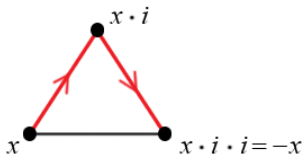

Figure 11. Impossible situation in a Grünbaum colored triangulation.

Finally, we give a geometric interpretation of Theorem 2 which will be useful in the future research. In fact, the 12 toroidal vertex-labeled triangulations, stated in Theorem 2, are realized geometrically as pairwise isometric noble toroidal 2-dimensional polyhedra in the 2-skeleton of the 16-cell in $\mathbb{R}^4$; see [**?**, **?**]; their difference as vertex-labeled toroidal triangulations ensures that the corresponding 12 polyhedra are different as point sets in $\mathbb{R}^4$. It would be interecting to identify explicitly the group of isometric transformations of $\mathbb{R}^4$ which move the 12 polyhedra one onto another.

Acknowledgment

The authors are indebted to Alex Law for assistance in preparing the diagrams of this paper.

References

[1] Harary, F. Graph Theory; Addison-Wesley: Reading, MA, 1969.

[2] Rosen, K. H. Discrete Mathematics and Its Applications, 4th ed.; McGraw-Hill: Boston, 2002.

[3] OEIS sequence A000055. URL: https://oeis.org/A000055

[4] Lang, S. Algebra, Revised 3rd ed.; Springer-Verlag: New York, 2002.

[5] Lawrencenko, S. Irreducible triangulations of the torus. (Russian); Ukrain. Geom. Sb. 1987, 30, 52–62.

[6] Lavrenchenko, S. A. Irreducible triangulations of a torus. J. Soviet Math. 1990, 51, 2537–2543.

[7] Lawrencenko, S. Polyhedral suspensions of arbitrary genus. Graphs Combin. 2010, 26, 537–548.

[8] Maslova, Yu. V.; Petrov, M. V. Lavrenchenko's polyhedron of genus one. In: Some Actual Problems of Modern Mathematics and Mathematical Education. (Russian); Herzen Readings - 2018 St. Petersburg (April 09-13, 2018), Russian Herzen State Pedagogical University. St. Petersburg, 2018, pp. 162-168.

[9] Boas, R. P., Jr. Inequalities for the derivatives of polynomials. Math. Mag. 1969, 42, 165–174.

[10] White, A. T. Graphs, Groups and Surfaces. North-Holland Mathematics Studies, No. 8; North-Holland Publishing Co., Amsterdam-London; American Elsevier Publishing Co., Inc., New York, 1973.

[11] Lawrencenko, S. Explicit lists of all automorphisms of the irreducible toroidal triangulations and of all toroidal embeddings of their labeled graphs. (Russian); Yangel Kharkiv Institute of Radio Electronics, Kharkiv (1987). Report deposited at UkrNIINTI (Ukrainian Scientific Research Institute of Scientific and Technical Information), report no. 2779-Uk87 (1 October 1987).

[12] Lavrenchenko, S. A. All self-complementary simplicial 2-complexes homeomorphic to the torus or the projective plane. Baku International Topological Conference. Abstracts. Part II (Baku, October 3–9, 1987) Baku, 1987. P. 159.

[13] Lawrencenko, S.; Vyalyi, M. N.; Zgonnik, L. V. Grünbaum coloring and its generalization to arbitrary dimension. Australas. J. Combin. 2017, 67 , 119–130.

Lawrencenko S.
E-mail: lawrencenko@hotmail.com
Russian State University of Tourism and Service,
Institute of Service Technologies,
99 Glavnaya Street, Cherkizovo, Pushkinsky District, Moscow Region, 141221, Russia

Magomedov A. M.
E-mail: magomedtagir1@yandex.ru
Dagestan State University,
Department of Discrete Mathematics and Informatics,
43-A Gadjieva, Makhachkala, 367000, Russia